Molecular Effects in H_2 Scattering from Metal Surfaces at Grazing Incidence

C. Díaz,* P. Rivière,† and F. Martín

Departamento de Química C-9, Universidad Autónoma de Madrid, 28049 Madrid, Spain

(Received 26 January 2009; revised manuscript received 22 May 2009; published 30 June 2009)

Collisions of fast atoms with surfaces at grazing incidence have been recently proposed as a promising new tool to determine surface parameters with unprecedented accuracy. Here we show, by means of classical dynamics calculations performed with first-principles six-dimensional potential energy surfaces for H_2/NiAl(110) and H_2/Pd(111) that, under grazing incidence conditions, fast light molecular projectiles are also useful to determine sticking probabilities at thermal energies, from the threshold up to the saturation limit. Thus they are the ideal complement to traditional experiments at thermal energies to determine sticking curves up to the saturation limit.

DOI: 10.1103/PhysRevLett.103.013201 PACS numbers: 34.35.+a, 68.49.Df, 82.65.+r

Atom scattering from clean alkali-halide surfaces at grazing incidence (1–3 degrees) and high collision energies (200 eV–25 keV) has been proposed in recent experiments [1–3] to investigate surface properties and decoherence phenomena. A striking observation is diffraction of the fast atomic projectile. Although diffraction of atoms and molecules was already observed in the 1930s [4], it was believed that it should disappear at high impact energy. On the one hand, this is because, at these energies, the corresponding de Broglie wavelength is much smaller than the typical surface lattice constant and, therefore, much smaller than the typical thermal displacement of the surface atoms (which introduces decoherence, thus hiding diffraction [5]). On the other hand, this is because a fast atom has enough energy to produce surface electron excitations and, hence, energy dissipation and decoherence [6]. Electronic excitations are negligible in wide band-gap insulators [7], but not necessarily so in metals. However, very recently, He diffraction has also been observed in experiments performed on Ag(110) [8] and on $c(1 \times 3)$S/Fe(110) and $c(2 \times 2)$O/Fe(110) [9], proving that the role of electronic excitations is not as dramatic as had been anticipated, at least for incidence energies smaller than 2 keV.

The physical phenomenon behind these remarkable experimental results is the strong decoupling between the fast motion along the incidence direction, parallel to the surface, and the slow motion perpendicular to the surface. Along the incidence direction (aligned with a symmetry direction with low Miller indices) the projectile moves in a periodic potential, which means that any acceleration is compensated by a slowing down, and therefore the momentum change along this direction, Δk_y, is zero. Any momentum change in the projectile is due to momentum transfer from the slow motion perpendicular to the surface (k_z) to the motion parallel to the surface and perpendicular to the incidence direction (k_x). The wavelength associated to this slow motion is comparable to the surface lattice constant, which leads to out-of-plane diffraction according to Bragg's law when Δk_x (the ''transverse momentum transfer'') coincides with a reciprocal lattice vector.

The above mechanism was proposed by Farías *et al.* [10] to explain experiments performed at much lower incidence energies ($E_i < 1$ eV). Using as a benchmark system the scattering of H_2 on Pd(111) at off-normal incidence, they showed that out-of-plane diffraction becomes dominant as the incidence angle θ_i (defined with respect to the surface plane) decreases and the incidence energy increases. Similar pronounced out-of-plane diffraction was observed in thermal scattering of H_2 on NiAl(110) [11] and Pt(111) [12]. Thus, scattering of fast atoms and molecules at grazing incidence was the natural test case for this mechanism.

The use of H_2 projectiles is not only interesting to learn about elastic diffraction but also to investigate intrinsic molecular effects such as rotationally inelastic diffraction [5] or dissociative adsorption on metallic surfaces [13]. At thermal energies these processes are relatively well understood, both theoretically and experimentally (see, e.g., [14–16] and references therein). At higher energies (>70 eV) and grazing incidence ($\theta_i \leq 10°$), molecular rovibrational excitation has been already studied [17,18]. Dissociation has been investigated in grazing incidence collisions of molecular ions that neutralize at the surface [19,20]. However, to our knowledge, dissociative adsorption of neutral molecules (which is the primary mechanism in heterogeneous catalysis) has never been investigated in fast grazing incidence conditions. In this Letter we present the results of six-dimensional (6D) classical dynamics calculations for the scattering of fast H_2 molecules from Pd(111) and NiAl(110) surfaces at grazing incidence, using 6D potential energy surfaces (PES) recently obtained from first-principles calculations [21,22]. The two systems are quite different: H_2/Pd(111) is nonactivated, i.e., H_2 can dissociate on the surface even at nearly zero incidence energy; H_2/NiAl(110) is activated and the threshold for dissociation is ~250 meV. We show that a plot of $1 - R$, where R is the total reflectivity, as a function of normal incidence energy $E_\perp$ practically reproduces the sticking

curves at thermal energies. This suggests that scattering of fast H_2 molecules at grazing incidence could be used as a complement to traditional sticking experiments to determine sticking curves from the threshold up to the saturation limit.

Previous theoretical studies of grazing incidence collisions of atoms [2,23,24] and molecules [17,18,20] on surfaces have made use of classical dynamics methods with model potential energy surfaces. Aigner *et al.* [25] have successfully used a quantum trajectory Monte Carlo method in combination with a potential energy surface (PES) obtained from first-principles for the He/LiF(110) system. A similar theoretical treatment for H_2 projectiles is substantially more involved. Thus, we have adopted a simpler approach that consists in performing classical trajectory calculations (also based on first-principles PESs) in combination with a binning method that accounts for the discrete changes in linear and rotational angular momenta. A classical trajectory is computed by solving the Hamilton equations of motion, and the probabilities are calculated as an average over the molecular initial conditions, which are obtained by using a classical Monte Carlo sampling method. This approach has led to sticking and rotationally elastic and inelastic diffraction probabilities at thermal energies in very good agreement with experiment for both H_2/Pd(111) and H_2/NiAl(110) [11,26]. The corresponding PESs were taken from [21,22], where they were determined by application of the corrugation reducing procedure [27] to a set of data from density functional theory calculations. Then, using these PESs, quasiclassical (classical) trajectory calculations, in which the initial vibrational zero point energy of H_2 is included (excluded), were performed. As described in [26], the intensity of a given diffraction peak with Miller indices (n, m) is evaluated as the fraction of trajectories in which the molecule scatters with a parallel momentum change contained in the 2D Wignez-Seitz cell built around the (n, m) lattice point in reciprocal space (see inset in Fig. 1). In view of the good performance of this binning at thermal energies, one can expect an even better performance at the higher incidence energies considered in this work. The final rotational state of the scattered molecules is obtained, depending on the parity imposed by the total nuclear spin of the molecule initial state, by evaluating the closest even or odd integer that satisfies $[-1 + (1 + 4L^2/\hbar^2)^{1/2}]/2$, where L is the classical angular momentum.

Classical (i.e., without binning) linear momentum transfer for $H_2(v = 0,\ J = 0)$ colliding with NiAl(110) along the crystallographic direction $[1\bar{1}0]$, for an incidence energy of 400 eV and incidence angle of 3° is shown in Fig. 1. The change in parallel momentum along the $[1\bar{1}0]$ direction is very small, much smaller than the reciprocal lattice constant, while the change in parallel momentum in the perpendicular direction is several times the reciprocal lattice constant. As can be seen, this behavior does not depend on the final rotational state of the molecule. Since all

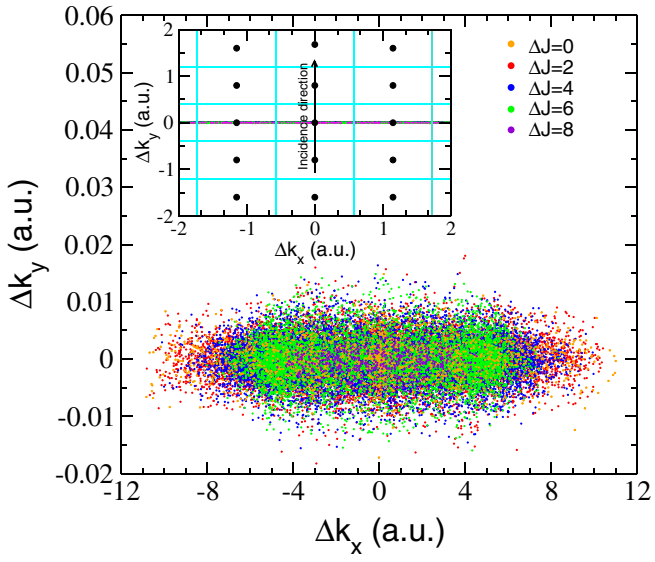

FIG. 1 (color online). Change in parallel momentum for $H_2(v = 0,\ J = 0)$/NiAl(110). The total incident collision energy is 400 eV, the incident angle is 3° and the crystallographic direction $[1\bar{1}0]$. The inset shows the same results superimposed to the NiAl(110) reciprocal lattice and the incidence direction. In this scale, the points form a thick horizontal line in the vicinity of $\Delta k_y = 0$.

variations in parallel momentum lie in the Wigner-Seitz cells centered in $\Delta k_y = 0$, one can already anticipate that, after binning, only out-of-plane diffraction perpendicular to the incidence direction in reciprocal space will be observed. Similar results are obtained for incidence along other symmetry directions with low Miller indices, as well as for H_2/Pd(111).

Calculated diffraction probabilities obtained after binning are presented in Fig. 2. The upper left panel shows results for $H_2(v = 0,\ J = 0)$ scattered by Pd(111) at an incidence energy $E_i = 400$ eV and an incidence angle $\theta_i = 1.25°$, and the upper right panel for H_2 scattered by NiAl(110) at $E_i = 400$ eV and $\theta_i = 3.0°$. In H_2/Pd(111), peak intensities decrease monotonically with diffraction order, while there is a clear intensity modulation in H_2/NiAl(110). A similar behavior is observed in the probabilities obtained with no binning (dotted lines in the upper panels of Fig. 2). Intensity modulations are well known in both thermal (see, e.g., [28]) and fast grazing elastic scattering [3,9] by surfaces containing two kinds of atoms (as, e.g., NiAl). Another characteristic of the NiAl(110) surface that contributes to this modulation is the presence of "buckling" [25], since, in this surface, the Al atoms are displaced upwards ($\delta Z = 0.174$ Å) with respect to the Ni atoms [22]. The lower panels of Fig. 2 show the corresponding diffraction spectra (θ, φ) that would be obtained in a typical experiment. In these spectra, diffraction peaks have been convoluted with a 2D Gaussian function of width σ. The diffraction peaks are organized in concentric circumferences that result from the approximate energy

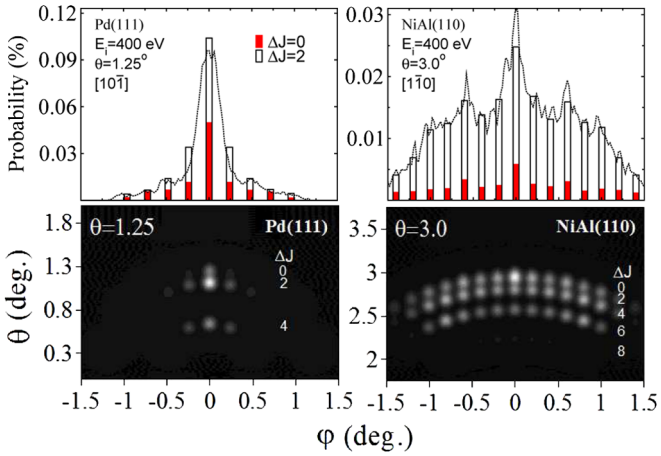

FIG. 2 (color online). Upper panels: probability of diffraction peaks as a function of φ for $H_2(v = 0,\ J = 0)$/Pd(111) (left) and $H_2(v = 0,\ J = 0)$/NiAl(110) (right), and 400 eV incidence energy. Dotted lines show the probabilities per degree ($\times 10$) without binning for $\Delta J = 2$. Lower panels: 2D (θ, φ) simulated diffraction spectra for the same conditions. θ is the angle between the scattering direction and surface plane and φ the angle between the projection of the scattering direction on the surface plane and the incidence direction. 2D results have been convoluted with a 2D Gaussian function of width $\sigma = 0.05°$ to simulate a typical experimental resolution.

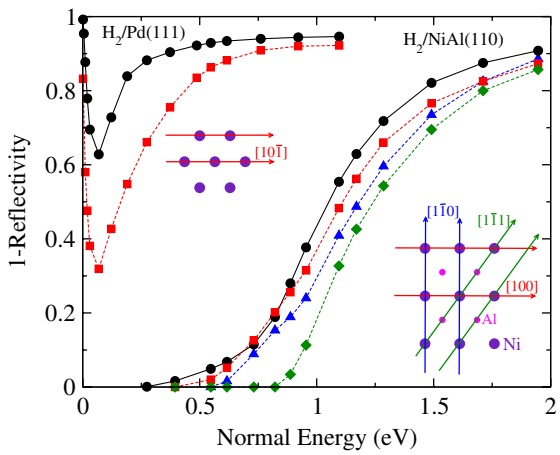

FIG. 3 (color online). $1 - R$, where R is the reflectivity, as a function of the collision normal energy (for $E_i = 400$ eV) for $H_2(v = 0,\ J = 0)$/Pd(111) and $H_2(v = 0,\ J = 0)$/NiAl(110). Black circles, (thermal) normal incidence results from Refs. [21,29], respectively, and red squares, fast grazing incidence along the crystallographic directions [10$\bar{1}$] and [100], respectively. Blue triangles and green diamonds: fast grazing incidence along the [1$\bar{1}$0] and [1$\bar{1}$1] directions, respectively, for $H_2(v = 0, J = 0)$/NiAl(110). The channel width is defined as the distance between nearest parallel rows of equivalent atoms along a given crystallographic direction (i.e., the distance between parallel lines with the same color in the insets).

conservation rule, $\Delta k_Z^2/2M + \Delta E_{\text{rot}} \simeq \Delta k_X^2/2M$. The upper semicircumference contains rotationally elastic peaks ($\Delta E_{\text{rot}} = 0$), the only peaks that would be observed in atomic diffraction [1–3,8,9]. The lower semicircumferences contain the rotationally inelastic diffraction peaks for $\Delta J = 2$ ($\Delta E_{\text{rot}} \approx 42$ meV), $\Delta J = 4$ ($\Delta E_{\text{rot}} \approx 141$ meV), etc. As the incidence angle (or $E_\perp$) increases, both the number of peaks in a given circumference and the number of semicircumferences increase. The same qualitative behavior is observed for both H_2/Pd(111) and H_2/NiAl(110), and for H_2 molecules initially in excited rotational states ($J > 0$). These theoretical spectra give an idea of what could be expected from a fast grazing molecular experiment.

Figure 3 shows the complementary of the total molecular reflectivity, $1 - R$, as a function of $E_\perp$ for $E_i = 400$ eV, $\theta_i = 0.1°$–$4.0°$ and various incidence directions, for both H_2/NiAl(110) and H_2/Pd(111). Surprisingly, the variation of $(1 - R)$ versus $E_\perp$ for fast grazing incidence looks very much like the corresponding sticking curves at thermal energies [21,29], both in shape and magnitude. For fast grazing incidence along the [100] direction of NiAl(110), the $1 - R$ curve is almost identical to the sticking curve at thermal energies. For the [1$\bar{1}$0] and [1$\bar{1}$1] incidence directions, the $1 - R$ curves are slightly shifted upwards in energy. This is a consequence of the collision dynamics. Indeed, the collision proceeds in a channeling regime [30]; i.e., the rows formed by the surface atoms guide the projectile in its motion along the surface. Channeling is poorer in narrow channels than in wide channels because, in the former, the projectile can more easily hit the potential walls and be scattered at the cost of parallel energy. Thus, in narrow channels, one can expect a larger reflectivity and that is why, as shown in Fig. 3, the wider the channel the less deviation from the sticking curve at thermal energies. Optimum channeling also explains why deviations decrease with increasing $E_\perp$. We have checked that, for the widest channel, the results remain unchanged within an interval of 0.5° around the incidence direction. Therefore, the optimum condition to obtain grazing $1 - R$ curves similar to sticking curves at thermal energies is to choose incidence directions associated with wide channels. The results for H_2/Pd(111) shown in Fig. 3 confirm this interpretation: the level of disagreement between the sticking curve at thermal energies and that of $1 - R$ at grazing incidence is similar to that found in NiAl(110) along the [1$\bar{1}$1] channel, which has a similar width. In Pd(111), the grazing incidence calculations even reproduce the nonmonotonic behavior of the sticking curve at thermal energies. We also note that the widest channel in Pd(111) is half of the widest channel in NiAl(110) (see inset Fig. 3), which means that, in Pd(111), one cannot obtain the correct sticking curve by just changing the incidence direction.

The above conclusion is independent of the total incidence energy chosen to obtain the $1 - R$ curves. Figure 4 shows the variation of $1 - R$ with $E_\perp$ for different values of the total incidence energy. As can be seen, the $1 - R$ curves are practically identical and, therefore, very similar to the sticking curve obtained at thermal energies. This is so in a wide range of incidence energies, 0.2–2 keV.

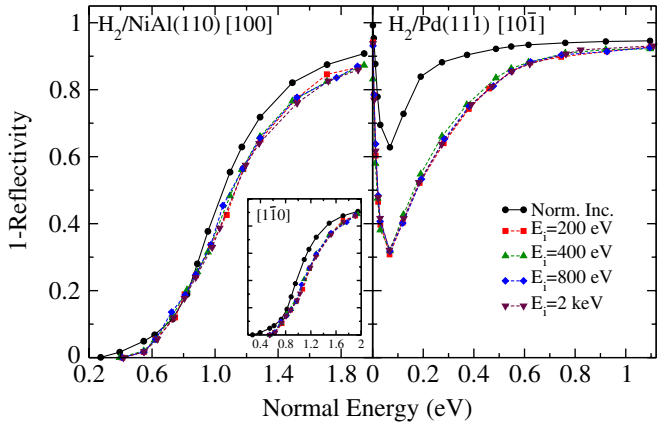

FIG. 4 (color online). $1 - R$, where R is the reflectivity, as a function of the collision normal and total (E_i) energy for $H_2(v = 0,\ J = 0)$/NiAl(110) and $H_2(v = 0,\ J = 0)$/Pd(111). Black circles, (thermal) normal incidence results from Refs. [21,29], respectively. Red squares, green triangles up, blue diamonds and maroon triangles down, fast grazing incidence at $E_i = 200$ eV, 400 eV, 800 eV and 2 keV, respectively.

Although the present results have been obtained for H_2 molecules in the lowest rovibrational state ($v = 0$, $J = 0$), explicit calculations for rotationally and vibrationally excited molecules show that the agreement between the corresponding sticking curve at thermal energies and the $1 - R$ curve vs normal energy obtained at grazing incidence is similarly good [31]. Therefore, determination of the $1 - R$ curves vs normal incidence energy provides a good estimate of the sticking curves at thermal energies irrespective of the degree of rotational and vibrational excitation of the incoming H_2 beam.

In conclusion, one can expect that, for rather open surfaces, measuring the molecular reflectivity in collisions of fast grazing H_2 molecules with surfaces can provide a good estimate of the corresponding sticking curve at thermal energies. The ideal candidates are alloys, like NiAl, in which one of the atoms barely contributes to surface corrugation, and superstructures adsorbed on metal surfaces, like (1×3)S/Fe(110) and (2×2)O/Fe. Such experiments could be used as a complement to traditional sticking experiments, which are technically limited to very low collision energies [32,33], usually lower than those needed to reach the sticking saturation values. This is relevant because, as shown in Refs. [29,34], extrapolation of low-energy sticking data can lead to wrong saturation values.

We are very grateful to H. F. Busnengo and D. Farías for useful discussions. We thank Mare Nostrum BSC and CCC-UAM for allocation of computer time. Work partially supported by the DGI Project No. FIS2007-60064 and CSD Project No. 2007-00010, the AECI Projects No. A/3067/05 and No. A/4722/06, the BSCH-UAM agency, the CAM Project No. S-0505/MAT/0194, and the program "Juan de la Cierva" (C. D.) from MICINN.

*cristina.diaz@uam.es
†Present address: Max Planck Institute for the Physics of Complex Systems, Nöthnitzer Str. 38, 01187 Dresden, Germany.

[1] A. Schüller, S. Wethekam, and H. Winter, Phys. Rev. Lett. **98**, 016103 (2007).
[2] P. Rousseau, H. Khemliche, A. G. Borisov, and P. Roncin, Phys. Rev. Lett. **98**, 016104 (2007).
[3] A. Schüller and H. Winter, Phys. Rev. Lett. **100**, 097602 (2008).
[4] I. Estermann and O. Stern, Z. Phys. **61**, 95 (1930).
[5] D. Farías and K. H. Rieder, Rep. Prog. Phys. **61**, 1575 (1998).
[6] P. M. Echenique, R. M. Nieminen, and R. H. Ritchie, Solid State Commun. **37**, 779 (1981).
[7] H. Winter, Phys. Rep. **367**, 387 (2002).
[8] N. Bundaleski, H. Khemliche, P. Soulisse, and P. Roncin, Phys. Rev. Lett. **101**, 177601 (2008).
[9] A. Schüller, M. Busch, S. Wethekam, and H. Winter, Phys. Rev. Lett. **102**, 017602 (2009).
[10] D. Farías *et al.*, Chem. Phys. Lett. **390**, 250 (2004).
[11] D. Farías *et al.*, Phys. Rev. Lett. **93**, 246104 (2004).
[12] P. Nieto *et al.*, Science **312**, 86 (2006).
[13] H. A. Michelsen, C. T. Rettner, and D. J. Auerbach, *Springer Series in Surface Science*, edited by R. J. Madix (Springer-Verlag, Berlin, 1994), Vol. 34.
[14] G. R. Darling and S. Holloway, Rep. Prog. Phys. **58**, 1595 (1995).
[15] A. Gross, Surf. Sci. Rep. **32**, 291 (1998).
[16] G. J. Kroes, Prog. Surf. Sci. **60**, 1 (1999).
[17] U. van Slooten, E. J. J. Kirchner, and A. W. Kleyn, Surf. Sci. **283**, 27 (1993).
[18] U. van Slooten and A. W. Kleyn, Chem. Phys. **177**, 509 (1993).
[19] M. Hamhami *et al.*, Nucl. Instrum. Methods Phys. Res., Sect. B **266**, 3359 (2008).
[20] I. Wojciechowski *et al.*, J. Phys. Chem. B **106**, 8233 (2002).
[21] H. F. Busnengo *et al.*, J. Chem. Phys. **116**, 9005 (2002).
[22] P. Rivière, H. F. Busnengo, and F. Martín, J. Chem. Phys. **121**, 751 (2004).
[23] Z. J. Fang, W. M. Lau, and J. W. Rabalais, Surf. Sci. **581**, 1 (2005).
[24] F. Gou, M. A. Gleeson, J. Villette, and A. W. Kleyn, Nucl. Instrum. Methods Phys. Res., Sect. B **247**, 244 (2006).
[25] F. Aigner *et al.*, Phys. Rev. Lett. **101**, 253201 (2008).
[26] C. Díaz *et al.*, J. Chem. Phys. **122**, 154706 (2005).
[27] H. F. Busnengo, A. Salin, and W. Dong, J. Chem. Phys. **112**, 7641 (2000).
[28] G. Boato *et al.*, J. Phys. C **6**, L394 (1973).
[29] P. Rivière, H. F. Busnengo, and F. Martín, J. Chem. Phys. **123**, 074705 (2005).
[30] D. S. Gemmell, Rev. Mod. Phys. **46**, 129 (1974).
[31] C. Díaz, P. Rivière, and F. Martín (to be published).
[32] M. Beutl, K. D. Rendulic, and G. R. Castro, J. Chem. Soc., Faraday Trans. **91**, 3639 (1995).
[33] C. Rettner, D. J. Auerbach, and H. A. Michelsen, Phys. Rev. Lett. **68**, 1164 (1992).
[34] M. F. Somers *et al.*, Chem. Phys. Lett. **360**, 390 (2002).